Environ. Sci. Technol. **1999**, *33*, 96−103

Biodegradation during Contaminant Transport in Porous Media. 2. The Influence of Physicochemical Factors

MARK L. BRUSSEAU,*,†,‡ MAX Q. HU,†,§ JIANN-MING WANG,† AND RAINA M. MAIER†

Soil, Water and Environmental Science Department and Hydrology and Water Resources Department, 429 Shantz, University of Arizona, Tucson, Arizona 85721

The biodegradation of contaminants in the subsurface has become a topic of great interest. In systems wherein biodegradation is coupled with transport, the magnitude and rate of biodegradation is influenced not only by microbial properties but also by physicochemical properties. The purpose of this work is to systematically evaluate the impact of coupled physicochemical factors (residence time, substrate concentration, and electron-acceptor concentration) on the biodegradation of contaminants during transport in porous media. A suite of miscible-displacement experiments was conducted with different residence times and initial contaminant concentrations, using a petroleum-contaminated aquifer material and benzoate as a model compound. The results were evaluated using a framework developed from a mathematical analysis of the nondimensional parameters that control biodegradation during transport. The results show that the type of transport behavior observed is dependent upon system conditions and is predictable using the controlling-parameter approach. For benzoate, which is a relatively labile compound, transport was measurably influenced by biomass growth under most conditions tested, albeit to different extents. The exceptions occurred when either the substrate or oxygen (electron acceptor) concentrations were limiting. The results obtained from this study should improve our understanding of the coupled influence of residence time, substrate concentration, and microbial properties on the biodegradation of contaminants during transport in the subsurface.

Introduction

The biodegradation of contaminants in the subsurface has become a topic of great interest. Knowledge of biodegradation processes is especially critical to the accurate prediction of contaminant transport, to conducting effective risk assessments, and to the development of successful in situ bioremediation systems. Clearly, these endeavors require an understanding of the factors that influence biodegradation under the dynamic conditions associated with subsurface systems.

* Corresponding author phone: 520-621-3244; fax: 520-621-1647; e-mail: brusseau@ag.arizona.edu.
† Soil, Water and Environmental Science Department.
‡ Hydrology and Water Resources Department.
§ Current address: Lawrence Berkeley National Laboratory.

In systems wherein biodegradation is coupled with transport, the magnitude and rate of biodegradation is influenced not only by microbial properties but also by physicochemical properties such as hydrodynamic residence time, substrate concentration, and electron-acceptor concentration. For example, the impact of residence time on biodegradation was examined in laboratory experiments reported by Angley et al. (*1*), Estrella et al. (*2*), and Kelsey and Alexander (*3*). They observed greater biodegradation at lower pore-water velocities and for longer columns, which was attributed to the longer period of contact between the substrate and the microorganisms. Several authors have used mathematical models to examine the impact of dispersion, oxygen availability, and other factors on biodegradation during transport (*4*−*13*). However, very few experiment- or modeling-based studies have explicitly examined the influence of several, coupled physicochemical factors on biodegradation of contaminants during transport.

The purpose of this paper is to present an experiment-based analysis of the impact of hydrodynamic residence time, substrate concentration, and electron-acceptor concentration on the biodegradation and transport of dissolved contaminants in porous media. An aquifer material collected from a fuel-contaminated site is used in the study, with benzoate selected as the model biodegradable compound. The results obtained from batch and miscible-displacement experiments are evaluated using a framework developed from a mathematical analysis of the nondimensional parameters that control biodegradation during transport.

Theory

Governing Equations. The nondimensional equations governing advective and dispersive transport of solute influenced by linear, instantaneous sorption, nonlinear biodegradation, biomass growth and decay, and electron-acceptor availability for one-dimensional steady-state flow are (*14*)

$$R\frac{\partial C^*}{\partial T} = -\frac{\partial C^*}{\partial X} + \frac{1}{P}\frac{\partial^2 C^*}{\partial X^2} - \epsilon_c M^*\left(\frac{C^*}{K_c^* + C^*}\right)\left(\frac{O^*}{K_o^* + O^*}\right) \quad (1)$$

$$\frac{\partial M^*}{\partial T} = \epsilon_m M^*\left(\frac{C^*}{K_c^* + C^*}\right)\left(\frac{O^*}{K_o^* + O^*}\right) - B(M^* - M_o^*) \quad (2)$$

$$\frac{\partial O^*}{\partial T} = -\frac{\partial O^*}{\partial X} + \frac{1}{P}\frac{\partial^2 O^*}{\partial X^2} - \epsilon_o M^*\left(\frac{C^*}{K_c^* + C^*}\right)\left(\frac{O^*}{K_o^* + O^*}\right) \quad (3)$$

where coefficients and parameters are defined in the Glossary, and where the following dimensionless parameters are defined as

$$X = \frac{x}{L}, \quad T = \frac{tv}{L}, \quad P = \frac{vL}{D} \quad (4)$$

$$C^* = \frac{C}{C_0}, \quad O^* = \frac{O}{O_o}, \quad M^* = \frac{M}{M_o} \quad (5)$$

$$\epsilon_c = \frac{\mu_m L M_o}{vYC_0}, \quad \epsilon_o = \frac{\gamma_o \mu_m L M_o}{vO_o}, \quad \epsilon_m = \frac{\mu_m L}{v} \quad (6)$$

$$K_c^* = \frac{K_c}{C_0}, \quad K_o^* = \frac{K_o}{O_o}, \quad R = 1 + \frac{\rho}{\theta}K_d \quad (7)$$

10.1021/es980311y CCC: $18.00
Published on Web 11/12/1998

The initial relative concentrations of substrate, oxygen, and biomass are 0, 1, and 1, respectively, in the domain. The upgradient boundary condition is given by

$$C^* = -\frac{1}{P}\left(\frac{\partial C^*}{\partial X}\right)_{X=0} = C_0^* \tag{8}$$

with $C_0^* = 1$ for $0 < T \leq T_0$ and $C_0^* = 0$ for $T > T_0$, where T_0 is the duration of the pulse input (in nondimensional time or pore volumes). The downgradient boundary condition is given by

$$\left(\frac{\partial C^*}{\partial X}\right)_{X=L} = 0 \tag{9}$$

The Monod equation is used to represent biomass growth and substrate (contaminant) biodegradation. This equation has been widely used for simulating biodegradation in batch systems (*15*) and is used often for coupling biodegradation and transport (*16*). The substrate is assumed to be bioavailable and the biomass is assumed to be immobile. Limitations associated with these and other assumptions will be discussed below.

The advantage of using the dimensionless form of the equations is that the number of independent parameters in the system is minimized. As will be shown below, three characteristic controlling parameters, χ, ϵ_m and K_c^*, are introduced through the dimensionless approach and represent the relative substrate-utilization coefficient, the effective maximum specific growth rate, and the relative half-saturation constant, respectively. These parameters reflect the combined effect of flow rate, path length, chemical, physical, microbial properties, and the boundary and initial concentrations of substrate and microorganisms in the system.

The ϵ_m is the effective maximum specific growth rate for microorganisms, which is a function of residence time t_r and maximum specific growth rate μ_m. The longer the residence time and the larger the maximum specific growth rate, the higher the effective maximum growth rate. The ϵ_c parameter is the apparent biodegradation rate coefficient, which is equal to $\epsilon_m\chi$, where χ, the relative substrate-utilization coefficient, is defined as

$$\chi = \frac{M_0}{YC_0} = \frac{\Delta C^*}{\Delta M^*} \tag{10}$$

The relative substrate-utilization coefficient can be viewed as the amount of initial biomass present in the system compared to the supply of substrate. Alternatively, it can be considered an inverse nondimensional yield coefficient.

Substrate degradation and biomass growth are both controlled by the term $C^*/(K_c^* + C^*)$, where K_c^*, the relative half-saturation constant, is the dimensional half-saturation constant normalized by substrate input concentration. This parameter indicates the affinity of the microbial population to the substrate, relative to the supply of substrate. The larger the relative half-saturation constant, the lower the substrate utilization and biomass growth rates.

Biodegradation with and without Biomass Growth. When modeling the transport of contaminants undergoing biodegradation, the latter process is often represented as first order. True first-order biodegradation will occur only in systems that have no net biomass growth. This may occur when the concentration of substrate, electron acceptor, or nutrients is too low to support net growth or when the rate of biomass loss (e.g., decay, outflux) is comparable to growth. When substrate transport is governed by first-order biodegradation (or any first-order mass loss process), the resultant breakthrough curves for continuous input conditions exhibit steady transport behavior, characterized by a constant plateau at a concentration that is less than the input concentration. Conversely, nonsteady transport behavior is observed when biodegradation is influenced by biomass growth. Specifically, the effluent substrate concentration decreases with time, even as solute is continually injected into the system. Furthermore, the maximum relative effluent concentration varies as a function of the input concentration when biomass growth influences biodegradation. This is not so for first-order mass loss, where the relative concentration at which the constant plateau occurs is the same, regardless of the initial concentration (e.g., a constant proportion of substrate is degraded for a first-order process, no matter the actual concentration).

The transport eqs 1−3 can be used to delineate conditions under which steady and nonsteady transport occur. The type of transport behavior observed depends on the magnitude of the three characteristic parameters ϵ_m, χ, and K_c^* discussed above. A diagram delineating expected transport behavior can be constructed using the effective maximum specific growth rate (ϵ_m) for the y axis, the relative half-saturation constant (K_c^*) for the x axis, and the relative substrate-utilization coefficient (χ) as the criterion for each "type curve" (see Figure 1). This "controlling-parameter" approach can be used to interpret and predict the transport behavior of biodegrading solutes (*14*).

To interpret and use this diagram, the location of the coordinate point corresponding to each experiment-specific pair of ϵ_m and K_c^* values is compared to the magnitude of the χ parameter (i.e., type-curve) associated with that experiment. If the coordinate point is greater than χ (i.e, if the point is above the type curve), the breakthrough curve should exhibit nonsteady behavior. Conversely, steady-state behavior (constant concentration plateau) should be observed when the coordinate point is below the type curve.

The greater effective maximum specific growth rates associated with larger values of ϵ_m will cause higher biomass growth rates and more biomass growth, which increases the amount of substrate degraded. This temporal increase in biomass concentration and associated biodegradation capacity produces a temporal increase in substrate demand, which results in nonsteady transport. Conversely, the minimal growth associated with lower ϵ_m values results in a relatively constant substrate demand and corresponding steady-state transport.

It is important to note that to maintain practicality with a focus on field applications, the type-curve diagram is based on relatively short-term behavior observed after the introduction or perturbation of a substrate pulse. Specifically, the focus is on the behavior exhibited during the first 20−25 pore volumes after introduction of a contaminant pulse. Thus, it must be stressed that the designation of steady-state transport obtained from use of the type curve may often apply only for some initial portion of the event. The duration of the steady-state phase will depend on the specific system conditions (*14*).

In the analysis presented above, the system was simplified to focus on the coupling between residence time, substrate supply, and biomass growth. The simplifications included assumptions that the substrate is readily available to the biomass, that nutrient and electron-acceptor concentrations are not limiting, that biomass decay is negligible, and that biomass is immobile. One or more of these assumptions are likely to be invalid in many cases, especially under field conditions. In such cases, the magnitude and rate of biomass growth and of biodegradation may be constrained, which would influence the associated transport behavior (*14*). For example, in a system constrained by electron-acceptor limitation, the concentration of electron-acceptor would be another factor controlling the biodegradation rate. In this case, the half-saturation constant of the electron-acceptor,

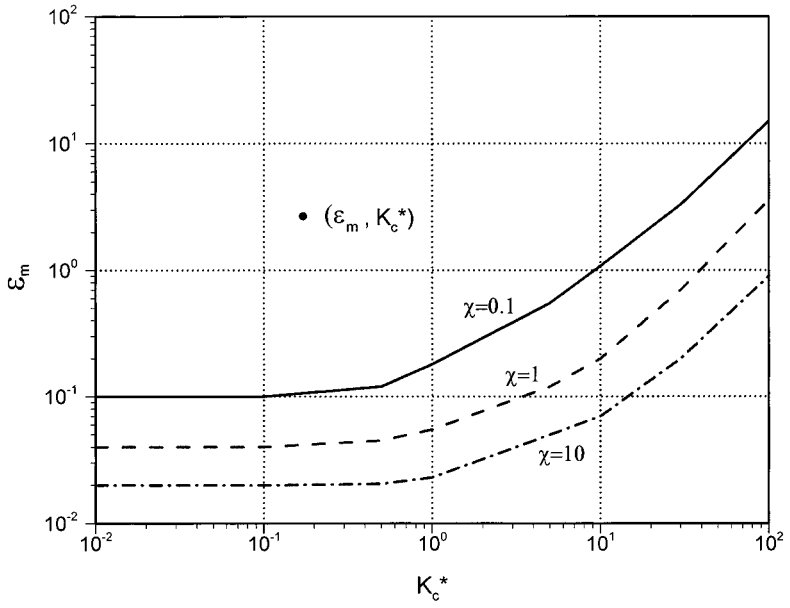

FIGURE 1. Type-curve diagram illustrating the influence of controlling factors on the type of transport observed. Steady transport is observed for the zone below a specific type curve and nonsteady transport above.

which indicates the affinity of the bacteria to the electron-acceptor, along with the electron-acceptor concentration would be an additional controlling factor. The higher the K_o, the greater the amount of electron-acceptor required for biomass growth, and the lower the biodegradation rate. Thus, the type curve would move upward and result in a smaller nonsteady transport zone.

Materials and Methods

Materials. Benzoate was selected as the model biodegradable solute (Aldrich Chem. Co., Milwaukee, WI). Benzoate is representative of the biodegradation of aromatic hydrocarbons such as alkylbenzenes, given it is an aromatic intermediate in the biodegradative pathway of many aromatic compounds. Benzoate is nonvolatile and should experience minimal hydrolysis under the system conditions. Thus, mass loss as a result of abiotic processes is unlikely. Given its physicochemical properties, benzoate is not expected to be sorbed by the aquifer material and thus should be readily available for biodegradation. Pentafluorobenzoate was used as the nonreactive, conservative tracer.

An aquifer material collected from a site contaminated by petroleum hydrocarbons was used for this study. This material is primarily sand (>96%), with a very low organic carbon content. The material was sieved prior to use to remove the particle-size fraction > 2 mm.

Laboratory Experiments and Data Analysis. *Degrader Enumeration*. The viable plate-count method was used to determine the number of benzoate degraders associated with the aquifer material. Suspensions were generated by adding 2 g of aquifer material to vials containing 9 mL of sterilized, distilled water and were vortexed prior to being serially diluted. Benzoate (1000 mg/L) was added to agar plates containing a Bushnell-HAAS mineral salts medium (Difco Laboratories, Detroit). The plates were then inoculated and incubated for 5 days prior to enumeration.

Batch Mineralization Experiments. The mineralization of benzoate was evaluated by quantification of $^{14}CO_2$ evolution. Aliquots (15 mL) of filter-sterilized benzoate stock solution made with mineral salts medium were added to modified 125-mL micro-Fernbach flasks (Wheaton, Milville, NJ). These flasks were then spiked with uniformly ring-labeled [^{14}C]-benzoate to obtain a specific activity of 0.89 μCi/mmol. After mixing, the flasks were inoculated with 2 g of soil. The experiments were conducted using seven initial concentrations of the substrate (0.01, 0.1, 1, 10, 30, 100, and 500 mg/L). Noninoculated flasks served as one set of controls, and flasks inoculated with sterilized (serial autoclaved) aquifer material served as another set of controls.

The flasks were incubated at room temperature on a gyratory shaker (Lab Line Orbit Shaker, Model 3527) at 200 rpm. A flushing-tree technique was used to periodically collect $^{14}CO_2$ (*2*). Concentrations of the evolved $^{14}CO_2$ as ^{14}C were determined by radioassay using a liquid scintillation counter (Packard Tri-Carb, Model 1600TR, Meriden, CT). The results from these experiments were used to calculate values for M_0, Y, μ_m, and K_c.

Miscible-Displacement Experiments. The apparatus and methods employed for the miscible-displacement studies with and without biodegradation were similar to those used previously in our laboratory (*17*, *18*). Preparative chromatography columns made of precision-bore stainless steel (2.1 cm i.d., and 7.0 cm in length, Alltech Associates Inc.) were used in the column experiments. The columns were sterilized (autoclaved) and then incrementally packed with air-dried porous media to obtain a uniform bulk density (1.77 g/cm^3). One HPLC pump (SSI Acuflow series II, Deerfield, IL) was connected to the column, with a three-way switching valve placed in-line to facilitate switching between solutions with and without the solute of interest. The packed columns were slowly wetted from the bottom to establish saturation (θ = 0.37), and approximately 100 pore volumes of synthetic groundwater were pumped through the column prior to use.

Experiments were conducted using various influent benzoate concentrations and pore-water velocities, as noted in the results section. The concentration of benzoate in the sterilized influent reservoir was monitored during the transport experiments to ensure constant C_0. In some cases, a flow-through, variable-wavelength UV detector (Gilson, Model 115, Middleton, WI) was used to continuously monitor concentrations of the compounds. Output from the detector was recorded on a strip-chart recorder (VWR Linear Chart Recorder). In other cases, when radiolabeled compounds were used, effluent was collected with a fraction collector and analyzed by radioassay. For the latter cases, the samples were analyzed before and after acidification to a pH < 2 to

differentiate between ^{14}C-labeled compound and $^{14}CO_2$. Selected samples were analyzed by HPLC to check for possible degradation intermediates, which were not found.

Precautions were taken to ensure that biodegradation was due solely to bacteria populations associated with the porous medium. All of the tubing for the column apparatus was sterilized by flushing with a 2% bleach solution. Afterward, the tubing was flushed with a 0.01% sodium−thiosulfate solution to neutralize the chlorine and then flushed with autoclaved, deionized water. In addition, an in-line filter (Whatman AQUEOUS IFD, 0.2 μm) was placed before the column inlet to prevent influx of particles (including bacteria).

Analysis of Batch Data. The results of the enumeration and mineralization experiments were used to calculate values for Y, M_0, μ_m, and K_c, which will be used in the analysis of benzoate transport. The initial biomass concentration was calculated with data collected from the plate-count experiments and the following equation

$$M_0 = \frac{\text{CFU}}{\text{g-drysoil}} \frac{9.5 \times 10^{-10}\ \text{mg-cellmass}}{\text{CFU}} \frac{\rho}{\theta} \frac{10^3\ \text{mL}}{\text{L}} \quad (11)$$

where CFU/g-drysoil is obtained from the plate counts (CFU = colony forming unit), the values for ρ and θ are from the column system, and the unit cell mass is obtained from ref *19*. The value for Y was calculated by converting the $^{14}CO_2$ data to the mass of cells produced, using $C_5H_7NO_2$ as the cellular composition, assuming that all benzoate was converted to either cell mass or CO_2. These assumptions were verified to be true for our system.

The $^{14}CO_2$ data were also used to determine substrate utilization over time for each initial substrate concentration. These data were used to calculate the specific growth rate (μ) for each initial substrate concentration, using

$$\mu_i = -m_i \frac{Y}{M_0} \quad (12)$$

where m_i is the maximum slope for each substrate utilization curve. The values for μ_m and K_c were obtained by plotting μ^{-1} versus C_0^{-1} from the inverse form of the Monod equation, where K_c/μ_m is the slope and μ_m^{-1} is the intercept.

Results and Discussion

Enumeration and Mineralization Experiments. The results of the viable counts, with benzoate as the sole carbon source, showed that bacteria capable of degrading benzoate exist in the porous media at levels of about 10^7 colony forming units per gram of material. As shown in Figure 2, $^{14}CO_2$ was evolved during the benzoate mineralization experiments, indicating benzoate can be mineralized by the indigenous bacterial populations. There was minimal lag in growth at the lowest substrate concentrations. However, lag appeared to increase with increasing substrate concentration, possibly due to toxicity effects. As described in the Materials and Methods section, the data were analyzed to calculate values for M_0, Y, μ, μ_m, and K_c, which are presented in Table 1.

Miscible-Displacement Experiments: Substrate and Oxygen Effects. The breakthrough curves for benzoate transport at the intermediate velocity (v = 23 cm/h; t_r = 0.3 h) are presented in Figure 3 for four influent concentrations. Benzoate exhibited no retardation, consistent with the fact that it is not sorbed by the aquifer material. The fronts of the breakthrough curves are relatively sharp and exhibit the same degree of dispersion as exhibited by pentafluorobenzoate, the nonreactive, conservative tracer (data not shown).

The effluent concentrations for benzoate experiments conducted using columns packed with sterilized aquifer material reached $C/C_0 = 1$ (data not shown). Conversely, the breakthrough curves obtained for the nonsterilized aquifer material do not reach a relative concentration of 1, which is the result of biodegradation. The results of the transport experiments indicate that benzoate generally exhibited nonsteady behavior. Specifically, the maximum relative effluent concentration is different for each C_0 experiment, with larger maximum effluent concentrations corresponding to larger influent concentrations. Furthermore, with the exception of the C_0 = 100 mg/L experiment, the effluent concentrations continue to decline, albeit at different rates, as solution is continuously pumped into the column. This behavior indicates biodegradation is influenced by biomass growth, as discussed in the theory section.

TABLE 1. Values for Microbiological-Related Parameters

initial biomass concn (M_0)	biomass yield (Y)	max. specific growth rate (μm)	half-saturation cons. (K_c)
63 mg/L	0.65	2.3 h^{-1}	20.4 mg/L
	specific growth rate (μ)		**specific growth rate (μ)**
C_0 = 0.01 mg/L	0.0009 h^{-1}	C_0 = 30	2.44
C_0 = 0.1	0.011	C_0 = 100	6.67
C_0 = 1	0.095	C_0 = 500	30.2
C_0 = 10	0.79		

The breakthrough curve obtained for C_0 = 1 mg/L exhibits a relatively small rate of decline, whereas the breakthrough curve for C_0 = 10 mg/L exhibits a larger rate of decline. These results are consistent with the relative magnitudes of K_c (20 mg/L) and C_0 for the two experiments. For the 1 mg/L experiment, C_0 is one-twentieth of K_c, which can create pseudo-first-order behavior, as can be seen from inspection of eq 2. For a given magnitude of ϵ_m (i.e., constant μ_m and t_r as implemented for these experiments), the growth rate will be reduced when K_c* is larger than one. When C_0 is much smaller than K_c, the rate of growth will be small, which results in a relatively constant rate of substrate utilization (see eq 1). This, in turn, results in a relatively constant concentration plateau, as seen for the C_0 = 1 experiments. Conversely, the larger rate of growth for the C_0 = 10 experiments results in a larger rate of increase in substrate utilization, which causes a larger rate of concentration decline. The results obtained for the slower (v = 2 cm/h) and faster (v = 120 cm/h) experiments (data not shown) are similar to the results obtained for the v = 23 cm/h experiments.

The breakthrough curves for the C_0 = 100 mg/L experiments for all three velocities exhibit constant plateaus (see Figure 3 for an example), even though this concentration is substantially larger than K_s. Evidence suggests that this was due to oxygen limitation. For the C_0 = 1, 10, and 30 mg/L experiments, the concentration of oxygen in the effluent was consistently greater than 1−2 mg/L. Conversely, the oxygen concentration was consistently below 1−2 mg/L for the C_0 = 100 experiments. This indicates that biodegradation was constrained by insufficient oxygen for the latter case, which limited cell growth and therefore resulted in the observation of pseudo-first-order behavior.

Miscible-Displacement Experiments: Residence-Time Effects. The breakthrough curves for benzoate transport with C_0 = 1 mg/L are presented in Figure 4a for three pore-water velocities, i.e., three residence times. The concentrations for all three curves exhibit relatively small rates of decline, indicative of pseudo-first-order biodegradation. This is related to the C_0-K_c effect, as discussed above. The magnitude of the plateau, however, varies with velocity. As discussed by Angley et al. (*1*), this phenomenon results from the dependency of the magnitude of biodegradation on the mean

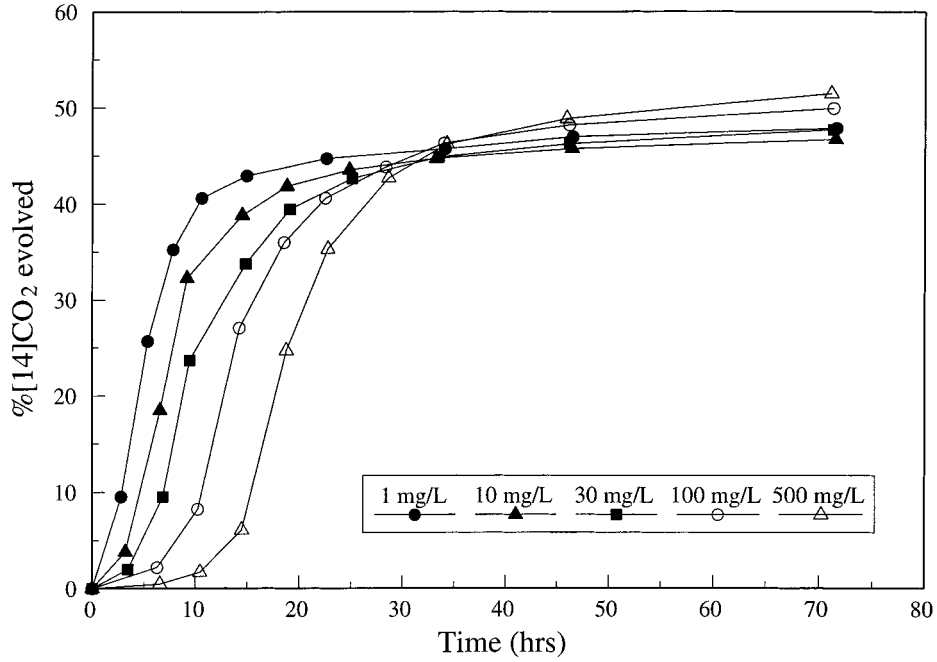

FIGURE 2. Evolution of $^{14}CO_2$ during biodegradation of benzoate for different initial concentrations.

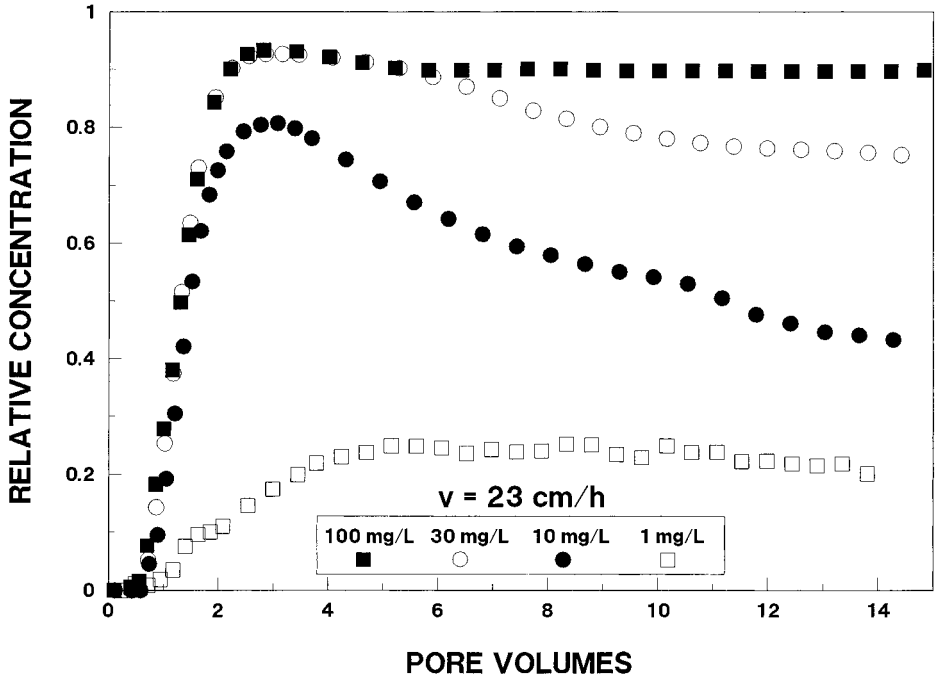

FIGURE 3. Breakthrough curves for medium-velocity transport of benzoate in aquifer material for four influent concentrations ($v = 23$ cm/h, $t_r = 0.3$ h).

contact time (i.e., residence time) between the substrate and the bacteria. This phenomenon is captured by the parameter ϵ_c defined in eq 6, which is a combination of the effective maximum specific growth rate and the relative substrate utilization coefficient. Inspection of eq 6 reveals that all coefficients comprising ϵ_c (μ_m, Y, M_0, C_0) are constant for this set of experiments, with the exception of t_r. Clearly, ϵ_c increases with increasing residence time, which results in greater substrate degradation and a lower relative effluent concentration (see eq 1).

The results obtained for the $C_0 = 10$ mg/L experiments, which are shown in Figure 4b, are a prototypical example of the impact of residence time on the transport of a substrate undergoing biodegradation influenced significantly by biomass growth. The magnitude of biodegradation was greatest for the largest residence time (smallest velocity) experiment, which indicates that the rate of biomass growth per pore volume of flow was greatest for this case. The relatively large rate of growth resulted in the breakthrough curve reaching a relative concentration of essentially zero, while benzoate solution was still being pumped into the column. Conversely, the breakthrough-curve plateau exhibits a much smaller rate of decline for the largest-velocity experiment, which indicates a much smaller rate of biomass growth per pore volume. In this case, the rate of biomass growth is constrained by the relatively short residence time. The breakthrough curve obtained for the intermediate velocity experiment exhibits intermediate behavior.

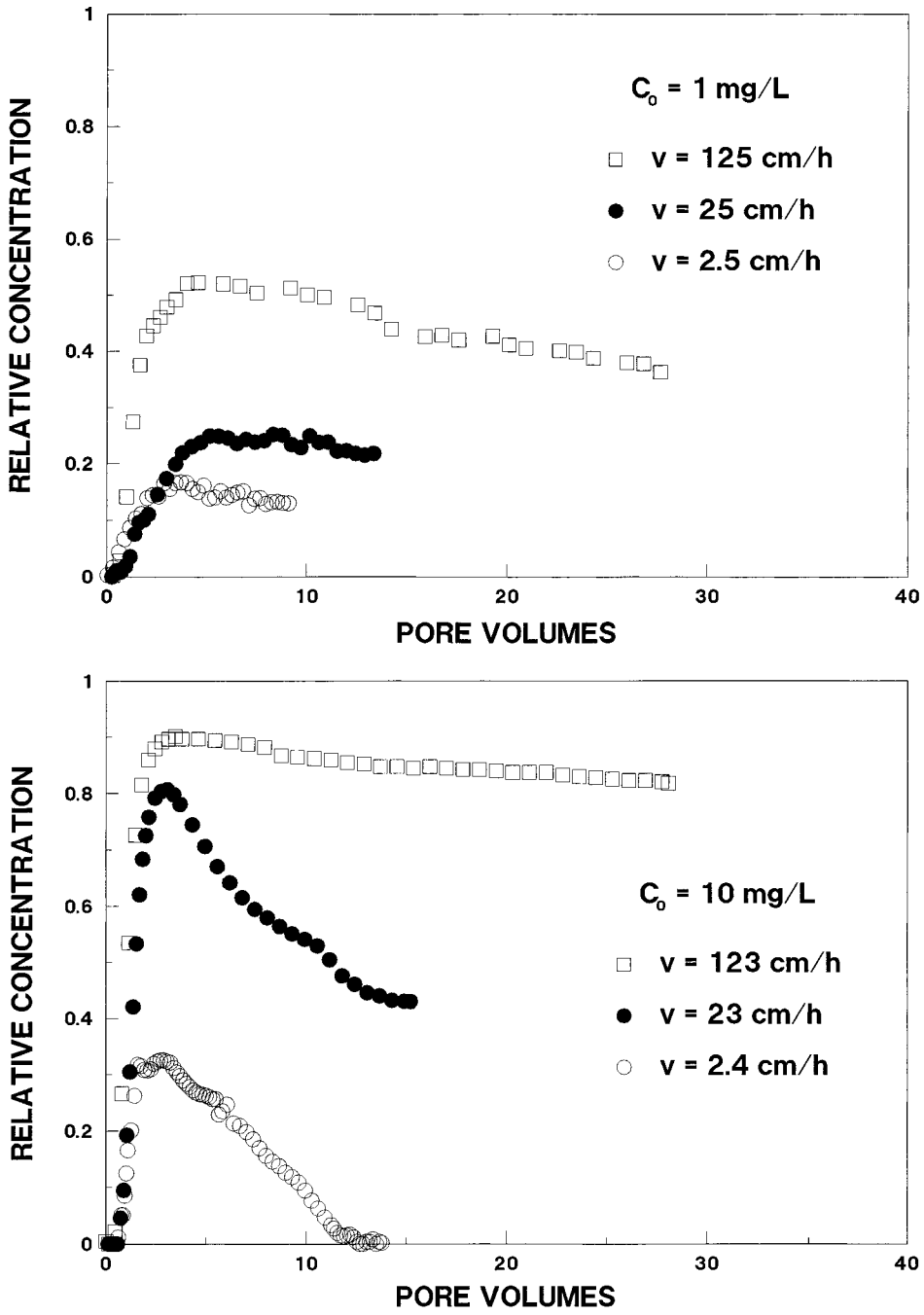

FIGURE 4. Breakthrough curves for transport of benzoate in aquifer material for three pore-water velocities: (A) $C_0 = 1$ mg/L; (B) $C_0 = 10$ mg/L; [$v = 125$ cm/h ($t_r = 0.058$ h), $v = 23$ cm/h ($t_r = 0.3$ h), and $v = 2.5$ cm/h ($t_r = 2.8$ h)].

The impact of residence time on the rate of biomass growth is defined by eq 2. The magnitude of ϵ_m is greater for larger residence times, which results in larger rates of growth. A larger rate of growth (i.e., greater rate of increase of M^*) produces a greater rate of increase in substrate degradation, as indicated by eq 1. Thus, the rate of decline of the breakthrough-curve plateau is larger for larger residence times.

Comparison of Measured Behavior to Theory. The results presented above may be evaluated using the controlling-parameter approach represented by Figure 1. To do this, the values for the three nondimensional controlling parameters, ϵ_m, K_c^*, and χ, were calculated for each miscible-displacement experiment. The pertinent microbiological-related parameters required for these calculations, Y, M_0, μ_m, and K_c, are reported in Table 1. The three physicochemical parameters required, pore-water velocity, column length, and C_0, are known for each experiment. The calculated values for the three nondimensional parameters are presented in Table 2.

Inspection of Table 2 reveals that, based on the theory, nonsteady transport behavior should be expected for nine of the 13 benzoate experiments reported herein. As noted in Table 2, nonsteady behavior was observed for all nine of these experiments. Conversely, steady-state behavior was expected, and observed, for the other four cases. For three of the four cases that exhibited steady-state transport, this behavior was due to oxygen constraints ($C_0 = 100$ mg/L benzoate). For the $C_0 = 0.1$ mg/L experiment, steady-state behavior was related to the large magnitude of K_c^* (~200), for which biomass growth would be negligible during the experiment. The consistency between the experiment and theory based results indicates that the controlling-parameter

TABLE 2. Controlling-Parameter Analysis of Transport Experiments

velocity	C_0	ϵ_m	K_c*	χ	coordinate location[a]	predicted behavior[c]	observed behavior[c]
2.3 cm/h	1	7	20.4	97	above	NS	NS
2.3	10	7	2.0	9.7	above	NS	NS
2.3	30	7	0.7	3.2	above	NS	NS[d]
2.3	100	7	0.2	1.0	$-O_2$[b]	S	S
23	1	0.7	20.4	97	above	NS	NS
23	10	0.7	2.0	9.7	above	NS	NS
23	30	0.7	0.7	3.2	above	NS	NS
23	100	0.7	0.2	1.0	$-O_2$[b]	S	S
172	0.1	0.09	204	969	below	S	S
123	1	0.13	20.4	97	above	NS	NS
123	10	0.13	2.0	9.7	above	NS	NS
123	30	0.13	0.7	3.2	above	NS	NS
123	100	0.13	0.2	1.0	$-O_2$	S	S

[a] Above = above type curve; below = below type curve. [b] $-O_2$ = biodegradation constrained by oxygen limitations. [c] NS = nonsteady transport; S = steady transport. [d] Breakthrough curve exhibited variable behavior (slightly nonsteady, followed by steady, and slightly nonsteady again).

theory adequately represented the coupled interactions between transport and biodegradation for our system.

With this work, we have attempted to systematically evaluate the impact of coupled physicochemical factors on the biodegradation of contaminants during transport in porous media. Clearly, the type of transport behavior observed will be very dependent upon both physicochemical and microbial properties. For benzoate, a relatively labile compound in this system (e.g., relatively large μ_m and M_0; relatively small K_c), transport was measurably influenced by biomass growth under most of the conditions tested, albeit to different extents. The importance of physicochemical factors was observed herein, as demonstrated by the influence of C_0, residence time and oxygen constraints on the magnitude and rate of benzoate biodegradation.

The results obtained from this study should improve our understanding of the coupled influence of residence time, substrate concentration, electron-acceptor constraints, and microbial properties on the biodegradation and transport of contaminants in the subsurface. The results should also help in the design and evaluation of in situ bioremediation systems. For example, it is clear that a substantial net growth of biomass will occur only under certain conditions. If these conditions are known, the system can be designed to attempt to promote growth and thus maximize performance.

Glossary

b	first-order biomass decay coefficient [1/T]
B	effective biomass decay rate coefficient [bL/v]
C	substrate (contaminant) concentration [M/L^3]
C*	relative substrate concentration [C/C_0]
C_0	substrate boundary input concentration [M/L^3]
D	hydrodynamic dispersion coefficient for substrate or electron acceptor [L^2/T]
K_d	equilibrium sorption coefficient [L^3/M]
K_c	half-saturation constant for substrate [M/L^3]
K_c*	relative half-saturation constant for substrate [K_c/C_0]
K_o	half-saturation constant for electron acceptor [M/L^3]
K_o*	relative half-saturation constant for electron acceptor [K_0/O_0]
L	characteristic (system) length [L]
M	biomass concentration [M/L^3]
M_0	initial biomass concentration [M/L^3]
O	electron-acceptor concentration [M/L^3]
O*	relative electron-acceptor concentration [O/O_0]
P	Peclet Number [vL/D]
q	Darcy velocity [L/T]
R	Retardation factor [$1 + \rho K_d/\theta$]
t	time [T]
t_r	residence time [L/v]
T	pore volumes or nondimensional time [tv/L]
v	pore-water velocity [L/T]
x	distance [L]
X	relative distance [x/L]
Y	yield coefficient for microorganisms [M/M] (biomass produced/mass of substrate degraded)
ϵ_c	effective substrate degradation rate coefficient [$\mu_m L M_0 (vYC_0)^{-1}$]
ϵ_m	effective biomass growth rate coefficient [μ_mL/v]
ϵ_o	effective electron acceptor consumption rate coefficient [$\gamma_0 \mu_m M_0 L (O_0 v)^{-1}$]
ρ	bulk density of porous medium [M/L^3]
μ	specific growth rate of microorganism [1/T]
μ_m	maximum specific growth rate of microorganism [1/T]
γ_0	stoichiometric coefficient equal to the mass of electron acceptor utilized by microorganisms per unit mass of "substrate" degraded
θ	fractional volumetric water content
χ	relative substrate utilization coefficient [M_0/YC_0]

Acknowledgments

This research was supported by a grant provided by the National Institute of Environmental Health Sciences, Superfund Basic Science Research Program.

Literature Cited

(1) Angley, J. T.; Brusseau, M. L.; Miller, W. L.; Delfino, J. *J. Environ. Sci. Technol.* **1992**, *26*, 1404−1410.
(2) Estrella, M. R.; Brusseau, M. L.; Maier, R. S.; Pepper, I. L.; Wierenga, P. J.; Miller, R. M. *App. Environ. Micro.* **1993**, *59*(12), 4266−4273.
(3) Kelsey, J. W.; Alexander, M. *Soil Sci. Soc. Am. J.* **1995**, *59*, 113−117.
(4) Borden, R. C.; Bedient, P. B. *Water Resour. Res.* **1986**, **22**, 1973−1982.
(5) Borden, R. C.; Bedient, P. B.; Lee, M. D.; Ward, C. H.; Wilson, J. T. *Water Resour. Res.* **1986**, *22*, 1983−1990.
(6) Celia, M. A.; Kindred, J. S.; Herrera, I. *Water Resour. Res.* **1989**, *25*, 1141−1148.
(7) MacQuarrie, K. T. B.; Sudicky, E. A. *Water Resour. Res.* **1990**, *26*, 223−239.
(8) MacQuarrie, K. T. B.; Sudicky, E. A.; Frind, E. O. *Water Resour. Res.* **1990**, *26*, 207−222.
(9) Molz, F. J.; Widdowson, M. A.; Benefield, L. D. *Water Resour. Res.* **1990**, *22*(8), 1207−1216.
(10) Sykes, J. F.; Soyupak, S.; Farquhar, G. J. *Water Resour. Res.* **1982**, *18*(1), 135−145.
(11) Widdowson, M. A.; Molz, F. J.; Benefield, L. D. *Water Resour. Res.* **1988**, *24*(9), 1553−1565.
(12) Chen, Y.-M.; Abriola, L.; Alvarez, P. J. J.; Anid, P. J.; Vogel, T. M. *Water Resour. Res.* **1992**, *28*, 1833−1847.
(13) Wood, B. D.; Ginn, T. R.; Dawson, C. N. *Water Resour. Res.* **1995**, *31*, 553−563.

(14) Brusseau, M. L.; Xie, L.; Li, L. *J. Contam. Hydrol.* **1999**, in press.
(15) Alexander, M.; Scow, K. M. Chapter 10 In *Reactions and Movement of Organic Chemicals in Soils*; Special Pub. No. 22, Soil Science Society of America: Madison, WI, 1989.
(16) Brusseau, M. L.; Rao, P. S. C.; Bellin, C. A. In *Interacting Processes in Soil Science, Advances in Soil Science*; Wagenet, J.; Baveye, P.; Stewart, B. A., Eds.; Lewis Pub.: Ann Arbor, MI, 1992; pp 147−184.
(17) Brusseau, M. L.; Jessup, R. E.; Rao, P. S. C. *Environ. Sci. Technol.* **1991**, *25*, 134−142.
(18) Hu, Q.; Brusseau, M. L. *Environ. Toxic. Chem.* **1998**, *17*, 1673−1680.
(19) Neidhardt, F. C.; Ingraham, J. L.; Schaechter, M. *Physiology of the Bacteria Cell, A Molecular Approach*; Sinauer Assoc. Inc.: Sunderland, MA, 1990; pp 506.

Received for review March 27, 1998. Revised manuscript received October 8, 1998. Accepted October 14, 1998.

ES980311Y